2020

Hardness and tensile properties of metals subjected to aging conditions

Talarico, P.M.; Kwon, Y.W.

Springer

Talarico, P. M., and Y. W. Kwon. "Hardness and tensile properties of metals subjected to aging conditions." Multiscale and Multidisciplinary Modeling, Experiments and Design (2020): 1-14.
http://hdl.handle.net/10945/65682

Multiscale and Multidisciplinary Modeling, Experiments and Design (2020) 3:187–200
https://doi.org/10.1007/s41939-020-00067-1

ORIGINAL PAPER

Hardness and tensile properties of metals subjected to aging conditions

P. M. Talarico[1] · Y. W. Kwon[1]

Received: 18 December 2019 / Accepted: 24 January 2020 / Published online: 19 February 2020

Abstract
Many metals used in engineering applications are exposed to aging conditions such as ultraviolet radiation and moisture. Aged metals are expected to lose their designed mechanical properties, and it was desired to relate a degraded local property to other homogenous properties. To study the aging effect, steel and aluminum were tested with reproduced variables in an accelerated weather testing chamber. Multiple tensile specimens of steel and aluminum were created to undergo accelerated Q-Lab Ultraviolet testing in the presence of radiation, heat and moisture. Accelerated aging resulted in decreasing surface hardness correlating with the tensile strength and elastic modulus for both steel and aluminum. The study also investigated the change in hardness through the depth of specimens resulting from aging, exhibited more consistently in steels. The overall strongest correlations existed in steels, between surface hardness and tensile strength, analogous to other studies. Modeling linear relationships for metal lifetime forecasts from hardness has been supported by this study. Outcomes can be expanded upon with more elaborate finite element analysis if desired in future experimentation.

Keywords Metals · Hardness · Micro-indentation · Aging condition

1 Introduction

The use of strong metal alloys for engineering design has been a standard practice for the marine industry. Groups of alloys that are most appropriate for wet environment structures are often classified as marine-grade metals. The design requirements of such metals are corrosion resistance with high tensile strength. Forecasting the reliability of structural designs is heavily reliant on accurate data for the behavior of mechanical properties. The capabilities to forecast mechanical properties accurately demand various techniques of evaluation. A desirable technique to explore is conventional indentation to analyze hardness, in pursuit of relationships to other mechanical properties changes (Leroux 2011; Smart and Bond 2016).

Relationships associated with environment aging and material property degradation are also useful to forecasting future property testing techniques (Craig 2005; Paul 2016). Hardness data collection is an established engineering practice and reliable technique that is predominantly used for intrinsic hardness characterization of materials. If an effort to accumulate similar data is extended to the relationship of tensile strength and elastic modulus parameters during metal again testing, a means to forecast long-term aging degradation in material properties may present itself, a method that would benefit various engineering research fields.

To guide and establish a set of test procedures, exposure testing specific, this research is concentrated on marine applications. To investigate metal aging appropriately, is it helpful to establish a specific structural model; one applicable naval vessel feature is the superstructure. Superstructures consist of varying thicknesses of plates regularly endure heat, water, and ultraviolet (UV) radiation (Tupper 2013). Common plating materials used in shipyards are aluminum and steel alloys, so that experimentation is extended to those alloys at varying thicknesses. Test procedures for exposure are advantageously set up for accelerated aging tests at substantial or excessive environment parameters for hopes of significant results. The intent on the monitoring properties of metallic samples before and after a series of tests will provide an early introduction into material life factors indicative of material property loss.

A similar framework of research, with micro-hardness as a forecasting factor, has surfaced periodically through vari-

✉ Y. W. Kwon
ywkwon@nps.edu

[1] Department of Mechanical and Aerospace Engineering, Naval Postgraduate School, Monterey, CA 93943, USA

ous professional research (Smart and Bond 2016; Nwokedi et al. 2018). It has not, however, had much focus on evolving relationships of hardness and mechanical properties. A common theme among research is test periods concentrating on surface coatings, and surface microstructure transformations (Li et al. 2011; Golumbfskie 2016). Though corrosion byproducts are relevant as an indication of an in-service failure manifestation, they may only serve as a reason to collect more robust micro-hardness data (Gouldstone 2007). Since mechanical properties like strength and modulus are based on the cross-sectional uniformity, findings may demand more procedure requirements if cross-sectional non-uniformity exists. Many of the hardness equations are derived from finite element analysis and geometric variations of hardness testing for projected relationships of mechanical properties to hardness (Nwokedi 2018; Kang et al. 2010). Illustrating similar linear relationships to other studies by means of time-dependent exposure experiment should encourage robust hardness examination for marine forecasting.

Ships are prepared for failure often by design early in the research and development phase of the acquisition life cycle, allowing time to set appropriate life cycle goals. The average life expectancy for a ship ranges from 20 to 30 years. In this lifetime, ships will spend a significant amount of the lifetime pier-side or in shipyards accumulating significant exposure to heat, UV radiation, and moisture.

Shipyard workers use various control practices to eliminate the prolonged contact of superstructure metals with water (Golumbfskie 2016). Preventative maintenance is a contemporary routine that is adopted by the personnel who conduct daily work on the in-service structures. Ultimately, maintenance is an abatement process to diminish the extent at which the alloys can be affected by irradiation, moisture, or other external variables. Test methods performed to forecast the sustainment of mechanical properties are adapted most appropriately by reproducing the environmental factors, such as temperature and irradiation.

Superstructures exhibit a highly observable surface where mechanical failures occur and, therefore, have become an area of interest to predict material life. Materials of interest used for this experiment are high-strength marine-grade 5456 Aluminum and A516 Carbon Steel. Each material was ordered in three thicknesses of plates and fabricated to American Standard for Test Methods (ASTM) E-8 plate specimen guidelines (ASTM 2016).

This paper investigated the change in hardness and mechanical properties in steel and aluminum resulting from the aging process and their correlation. In particular, the change in hardness was examined through the thickness of the specimens during the aging process. The paper consists of the following sections. The next section describes the experimental procedures, which was followed by the data collections. Then, analysis of results is presented followed by conclusions at the end.

2 Description of experiments

This section describes the methodical approach and milestones involved in the collection of aluminum and steel experimental data. Specific material types, size and specifications were used for sample classification. More scrutinizing data were collected as applicable if recorded data were suggestive of a new trend. Precedence of collection was data collection for exposure periods but not restrictive to bulk data collection at set intervals that did not illustrate changes. This helped to alleviate limitations of time and the extent of the research. This section also discusses the various test equipments used in the experiment with established settings or incorporated steps for recurring data integrity.

The materials used in this study were 5456 Aluminum and A516 Carbon Steel with three different thicknesses; 3.175 mm (1/8 in.), 4.763 mm (3/16 in.) and 6.35 mm (1/4 in.). These thicknesses were called ‘thin’, ‘standard’, and ‘thick’ in the following discussion. Both materials are considered high-strength alloys applicable for marine applications. Dog-bone shape coupons as specified in ASTM E-8 (ASTM 2016) were prepared out of those metal plates. Measurements of samples were then recorded as summarized in Tables 1 and 2.

2.1 Accelerated aging tests

The accelerated weathering test chamber utilized for this experiment was Q-Lab Ultraviolet (QUV) Tester condensation variant (85-cw) (QUV 2019). The test conditions were set at 1.55 W/m^2 UV using UVA lamps, 80 °C to maximize the accelerated results. One set of tests was continued for 90 h, and the tests were repeated for additional cycles.

Table 1 Measured specimen thickness of steel

Thickness	Average (mm)	Standard deviation (mm)
Thin	3.48	0.10
Standard	5.64	0.10
Thick	7.23	0.02

Table 2 Measured specimen thickness of aluminum

Thickness	Average (mm)	Standard deviation (mm)
Thin	3.13	0.02
Standard	4.83	0.07
Thick	6.45	0.05

Table 3 Exposure data collection periods

Name	Days	Hours
Baseline	0	0
Run 1	21	504
Run 2	60	1440
Run 3	100	2400
Run 4	140	3360

The test equipment was calibrated for two parts before testing. First, the UV sensors are calibrated by a CR10 radiometer procedure for each of the four main sensors, two in the front and two in the back. Calibration was completed and recorded in the QUV with no discrepancies. The second component of calibration is the temperature calibration. This was a temperature sensor and thermos of water at each of the temperature sensors in accordance with ASTM E-220. No discrepancies were found. Calibrations were conducted more than once, starting with this preliminary calibration. The follow-up calibrations were completed every 500 h of runtime for the UV and every 6 months for the temperature.

The QUV model utilized has the condensation variant of the test chamber. The heat is introduced through heated water and vapor from the bottom of the chamber base. It is constantly fed by a water feed and pump. The heating elements under the pan produce a condensation cycle by producing vapor that rises to the panel holders that form the side walls with the samples.

The standard panels were replaced by panels designed for tensile testing samples, each of which can hold three samples. Twelve panels are available on each side for completing samples. This allowed for three to six samples to be inserted for each combination of alloy and thickness. Since the accumulated run time is tracked, samples were able to be removed and replaced with blanks for hardness testing while other samples completed further exposure testing.

Completed batch runs were conducted over periods categorized as the following Table 3. Each run has a duration of ± 3 days due to withdrawal of samples for intermediate testing. Each sample had a specific value of exposure time recorded, if a circumstance required further investigation.

2.2 Hardness tests

Hardness testing was initially conducted on the surface of the specimen. Samples were set aside until cool to touch before any step was completed. Once cool, the samples were manually polished for 2 min with 1000 grit paper and 2000 grit paper and distilled water. If the specimen was only intended for intermediate hardness values and not destructive tensile testing, only one side of the sample was polished to support data integrity of cumulative surface effects.

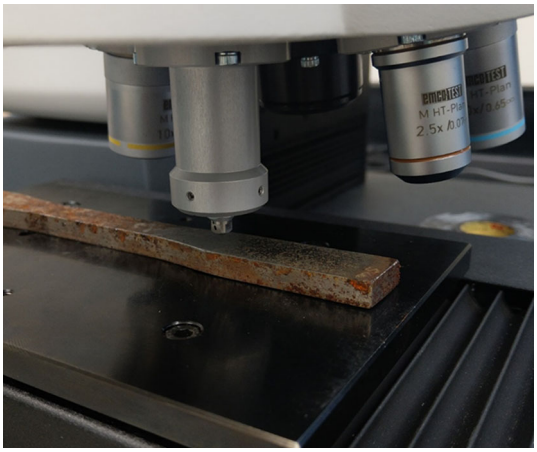

Fig. 1 Surface hardness data collection

Once the direct surface that was exposed was prepared, the specimen was brought to the Streurs Microhardness Tester. The current software that pairs with the indenter is eCOS Workflow V 2.2.3. The DuraScan model provides the capability to construct a series of local hardness data measures which supported the copious amount of data points that were collected for the surface hardness measures.

Setup and settings were completed in accordance with the DuraScan User's Manual and standard queries of the eCOS Software. Once data series is selected, the method for Vickers Hardness (HV3) was selected. Test load range for this hardness tester force is capable of macro- and micro-hardness results (use of above and below 1 kg force). The user's manual had suggested test loads and optical zoom for different materials. The following were used for each of the samples tested:

Aluminum samples: 40 × magnification and 0.3 kg load.

Steel samples: 40 × magnification and 0.5 kg load.

If a sample proved difficult to attain good marks, the operator adjusted the zoom as needed for manual repositioning. The samples were placed in the middle of the provided base with the exposed surface face up as shown in Fig. 1. After placement was set, the data collection is detailed at the computer.

The positioning of data collection start and spacing was entered into the data point editor to start hardness collection at the surface edge as shown in the square of Fig. 2. The spacing was 0.3 mm and moved in the direction across the width of each specimen. The width of the widest portion of the grip section was used for all samples; so, no stress concentrated would be created for later tensile testing.

Data from the surface hardness had early indications that the data should be organized by thickness of samples (later analyzed). Due to this, cross-sectional cuts were made in the same larger-width area to collect hardness values into the cross section.

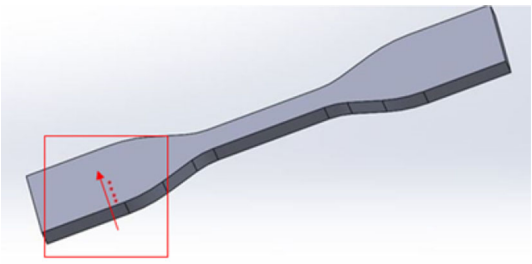

Fig. 2 Specimen drawing depicting hardness data point collection

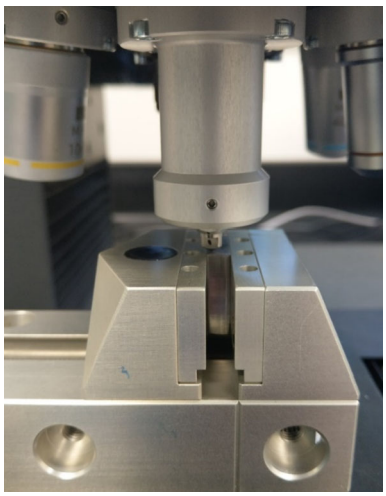

Fig. 3 Cross-section hardness collection

This method of collection required a clamp to set on the base and hold the cross section as shown in Fig. 3. Like the surface data, the surface was polished and staged in the computers point editor. For this collection, a closer representation of change was ideal; so, spacing was changed to 0.1 mm for every point moving away from the surface and into the material. There were fewer cross sections to complete this testing; so, a total of ten columns of data were collected with a spacing of 0.25 mm between each column, visualized in Fig. 4.

2.3 Tensile tests

Tensile testing is the test for specimen to acquire valid mechanical properties for the samples. Settings were entered to complete the uniform load increase until fracture with data collection at an interval of 10/s. Specimens are clamped on the grip section of the ASTM E8. The program completes a full tensile test load cycle until fracture occurs. The preliminary raw data curve for the tensile response can be read on the display during the process to monitor the test. From the test, elastic modulus and the ultimate strength were determined.

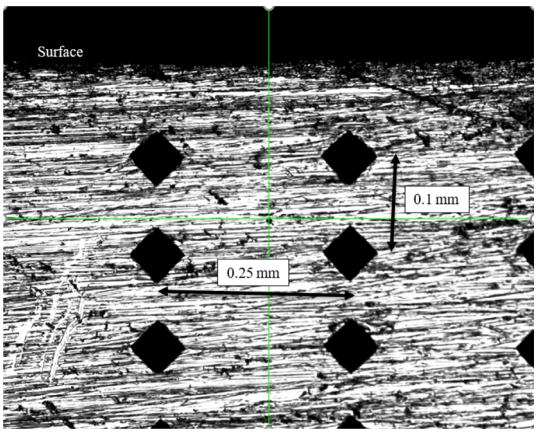

Fig. 4 Cross-section hardness test spacing

3 Data collection

3.1 Temperature, weight and visual inspection

Upon completion of an exposure period, batches were measured for temperature and weight. Temperature values had no significant deviation through iterative exposure testing. Temperatures were acquired by an infrared temperature gun. Since the gun is a point measurement, average temperature was collected up and down the samples. Aluminum was consistently read at 84 °C and steel was 74 °C. Temperatures did not vary sample to sample. Temperature ranged on each sample from up and down measurements differed no greater than 4 °C. The thin midsection of specimen was hotter than the top.

Weights of samples prior to testing was completed for every exposure period, see Table 4. Weight values were collected once specimens were dry and without cleaning the surface from the surface rust. The maximum weight gain was 0.3 g in a steel sample exposed 150 days. The aluminum samples saw no increase or decrease more than 0.03 g for the extent of the experiment. Aluminum, however insignificant, was the only alloy that had any specimen with weight losses.

Surface corrosion was visible as early as 21 days (run 1) on the steel samples. Verdigris became increasingly consistent across the entire surface and risen from the surface. Figure 5 shows a sequential-exposure picture of samples of steel and aluminum. The first two periods had more noticeable staining and pitting on steel samples since the corrosion did not cover the entire surface. Aluminum did not see noticeable changes in appearance. The physical appearance of thick and thin steel was not noticeable until exposure run 3. The difference in accumulated rust was not apparent on all thick and thin samples. Additional testing was completed on thick steel specimen, reaching a total exposure time of 150 days for run 4. The extent of corrosion was equally evident between run 3 and run 4.

Table 4 Dry weight data

Size	Baseline weight average (g)	Weight loss (%)			
		Run1	Run2	Run3	Run4
Steel weight loss change (g)					
Thin	94.91	0.03	0.03	0.04	
Standard	141.11	0.01	0.04	0.06	
Thick	186.22	0.01	0.00	0.05	0.13
Aluminum weight change (g)					
Thin	27.45	0.00	0.01	− 0.01	No Run 4
Standard	41.99	0.01	− 0.01	0.01	
Thick	55.78	0.00	0.00	− 0.02	

Fig. 5 Three sequential runs of exposure steel samples; left 21 days, center 60 days, right 100 days

3.2 Hardness data

All hardness tests were carried out in accordance with the procedure and equipment parameters described in the last section. Data were organized in excel after being recorded from the ECOS output on the computer. Each subset of data was organized by parameters including material, exposure time, and varying thickness. Data points were only collected from the side that was exposed to the irradiance in the QUV chamber. Due to testing procedures being cumulative in nature, some of the samples were tested and placed back in the chamber for more exposure. In the cases where this was done, only one end of the specimen was polished to leave the sample with one untarnished surface for secondary hardness testing after further exposure.

According to the data provided by the supplier of the materials for the Aluminum 5456-O plates, the Brinell Hardness is 90, which is equivalent to 94 on the Vickers hardness scale. This is consistent to the typical value for 5456-O of Vickers hardness. Due to the composition of the marine-grade high-strength alloy, there is likelihood these values will vary. Therefore, the only baseline (no exposure) data that will be utilized for this analysis are the values from untested specimen using the same equipment as the exposed specimen.

Table 5 tabulated the hardness of aluminum samples of three different thicknesses on their exposed surfaces for three different exposure runs on top of the baseline values. The results are also plotted in Figs. 6, 7 and 8. The test data showed the reduction in the hardness during the aging process.

According to the data provided by the supplier for the Steel A516 plates, the Brinell hardness is 147, which is equivalent to the same value in Vickers hardness. Table 6 and Figs. 9, 10 and 11 are the hardness of steel samples of three different thicknesses for four different exposure runs on top of the baseline data. All the hardness values were measured on the surfaces which were exposed to UVA.

Cross-sectional results were also collected and organized to help validate surface results and provide further analysis behind thickness contribution to hardness. Figure 12 depicts the pattern of cross-sectional hardness data collection. The data consist of eight rows of data points with 10 data points (columns) for each incremental step into the material away from the exposed surface. The first row of data is collected from the surface data because hardness data cannot be collected at the exact local point where the cross section meets the surface. Two of the most symptomatic hardness trends are shown in Tables 7 and 8 for the steel and aluminum samples.

The difference from surface measurement and first row on the cross section is the most significant. The difference was less evident for aluminum samples, and for steels it was consistently a 6–10 HV difference.

3.3 Mechanical property

The deliverables of tensile testing were strength and stiffness. Stress–strain plots were completed from the data of each individual specimen. Figure 13 shows the stress–strain plots of the standard size steel. The three curves displayed are the original baseline samples and two samples from the third

Table 5 Aluminum hardness data summary

Aluminum												
Thickness	Thin				Standard				Thick			
Exposure	Bline	Run1	Run2	Run3	Bline	Run1	Run2	Run3	Bline	Run1	Run2	Run3
Days	0	21	60	100	0	21	60	100	0	21	60	100
Std (HV)	2.87	1.78	2.02	1.92	2.42	2.48	2.03	1.60	2.18	1.90	1.75	2.22
Average (HV)	99.84	97.05	96.43	96.33	103.60	102.60	102.24	101.42	103.97	102.25	102.15	100.63
% loss		− 2.80	− 3.42	− 3.52		− 0.97	− 1.32	− 2.10		− 1.65	− 1.74	− 3.21

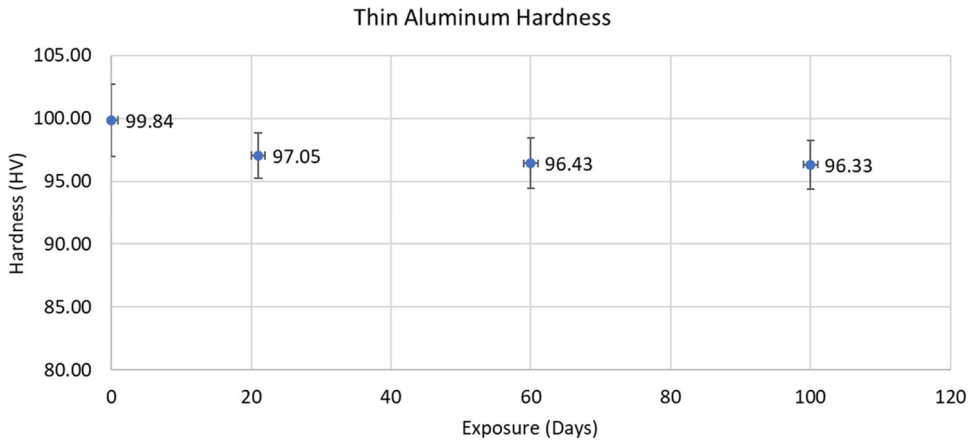

Fig. 6 Plot of hardness of thin aluminum samples

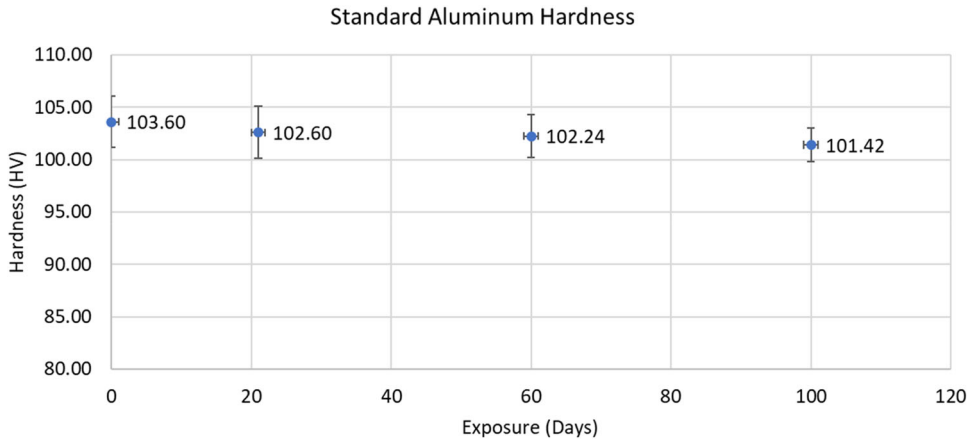

Fig. 7 Plot of hardness of standard aluminum samples

run of exposure. To show the change in ultimate strength, the plots were enlarged in Fig. 13b. It shows a small decrease in UTS. There is also no distinguishable difference in the elastic modulus. The thin steel sample stress–strain plots show similar results in that elastic modulus change is undistinguishable while UTS decreased by a small factor.

Figure 14 displays the stress–strain curves of thin aluminum samples. The plot shows the reduction in the UTS. The thick aluminum samples had the largest decrease in UTS. The change in UTS was tabulated in Tables 9, 10 and 11 for the aluminum samples. On the other hand, Tables 12 through 13 are for the steel samples.

4 Analysis of results

As annotated in the last section, sets of data showed varying relationships from test data. The preliminary organization of data was expected to be analyzed without much segregation by thickness. After the second exposure run the data already established trends that prescribed enough trends involving thickness as factor during exposure testing. The primary means of hardness testing, Vickers hardness on the surface, had distinguishing grouping by thickness. The difference was also apparent in the destructive testing UTS results. If thickness was not considered at start, the standard deviation would have been an issue with values of near 30 MPa UTS and 8

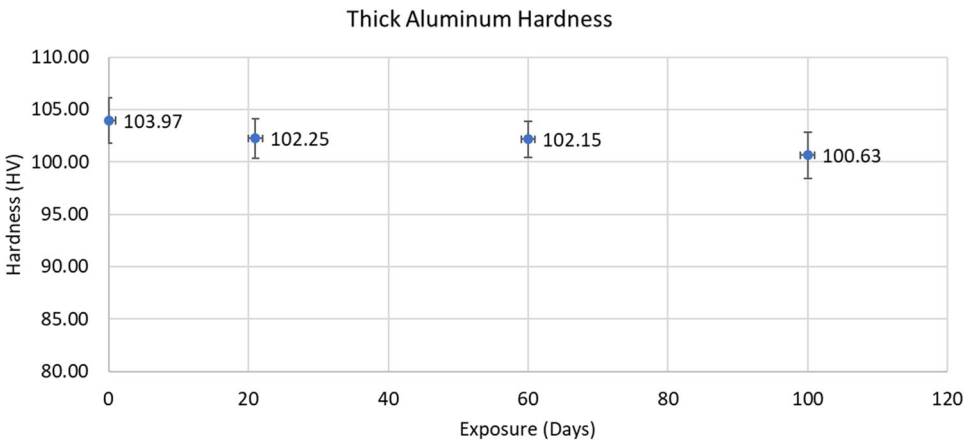

Fig. 8 Plot of hardness of thick aluminum samples

Table 6 Steel hardness data summary

Steel													
Thickness	Thin				Standard				Thick				
Exposure	Bline	Run1	Run2	Run3	Bline	Run1	Run2	Run3	Bline	Run1	Run2	Run3	Run4
Days	0	21	60	100	0	21	60	100	0	21	60	100	150
Std (HV)	5.68	5.25	5.41	4.68	5.12	4.35	4.51	4.96	5.36	4.68	3.10	3.87	4.86
Average (HV)	192.75	188.60	188.41	187.72	187.87	183.06	184.21	179.79	199.52	198.18	197.12	197.14	188.59
% loss		− 2.15	− 2.25	− 2.61		− 2.56	− 1.95	− 4.30		− 0.67	− 1.20	− 1.19	− 5.48

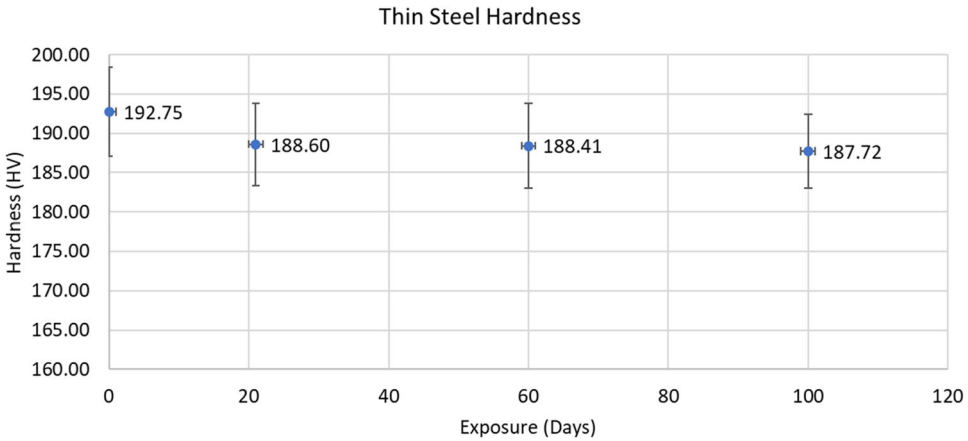

Fig. 9 Plot of hardness for thin steel samples

HV. Though the deviation in baseline samples served as a precaution to what factors are in effect, by segregating the data early, it resulted in favorable deviation by run 3 and run 4 data. A limitation of the methods and analysis was due to the possible natural occurrences that could have caused the deviation in data at the original state.

Both the extent of exposure and thickness of samples showed identifiable relationships for both steel and aluminum samples. Steel and aluminum began a small loss of strength and hardness properties as early as the first exposure testing period. Standard deviation started improving for all test by exposure period 2 (60 days). Due to this, the 60-day period is determined to be the first exposure period that has a loss in mechanical properties, even though steel showed rust on the surface much earlier. Due to available samples and the excessive weight gain of rust on steel, one last run of exposure proved the most vital. By exposing thick steel samples for an additional 50 days for a total of 150 days, the overall hardness loss surpassed five percent as shown in Table 6. This 150-day threshold is expected to hold valid for modeling but can be validated further by investigating microstructure with a scanning electron microstructure.

It was conclusive that surface interactions in the test environment initiated a change in hardness and visible failure mechanisms. In previous studies (Paul 2016; Lu et al. 2013), it was suggested that conventional hardness meth-

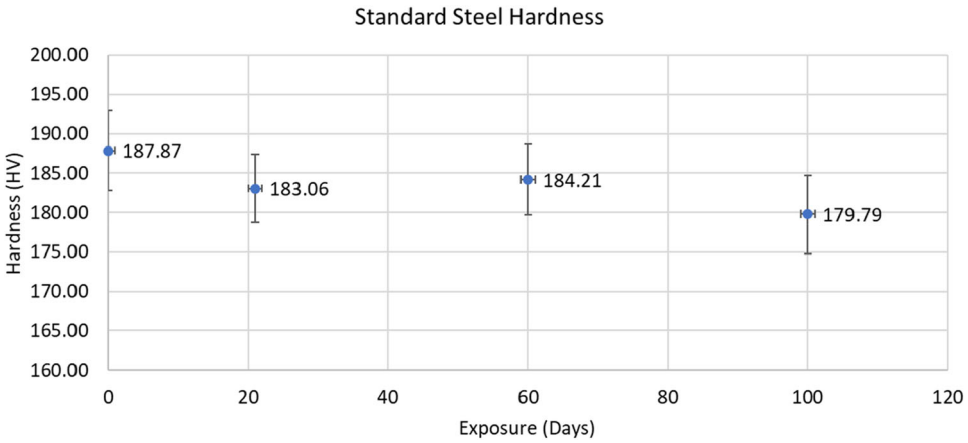

Fig. 10 Plot of hardness for standard steel samples

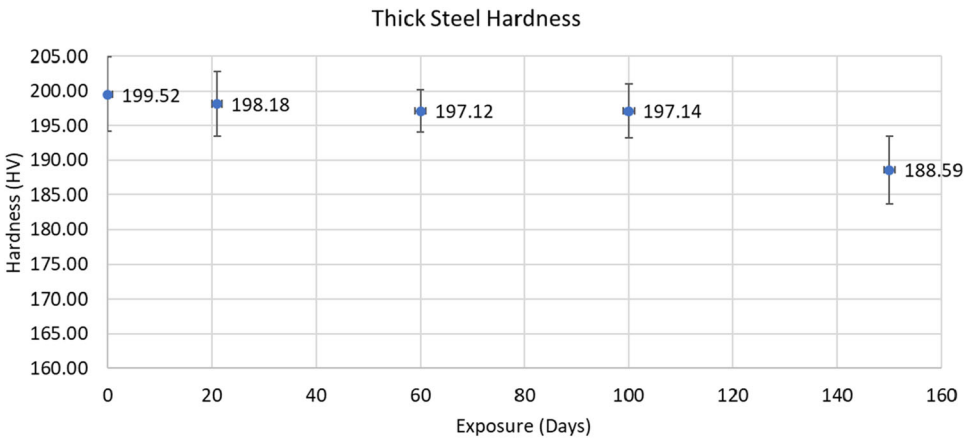

Fig. 11 Plot of hardness for thick steel samples

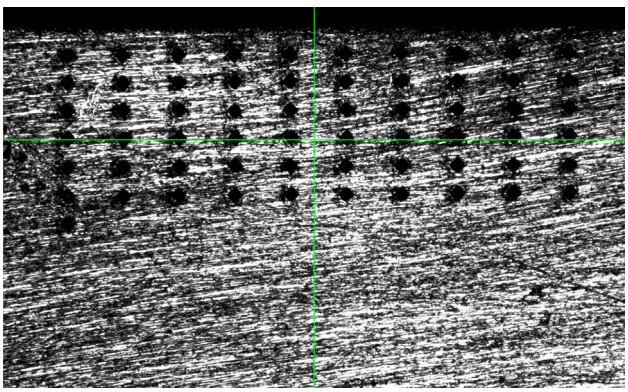

Fig. 12 Pattern of Hardness data points for cross-sectional analysis

ods could require depth-specific collection due the nature of grain heterogeneity and extent of accelerated weathering. The cross-section hardness tests presented some further detail to the extent of uniform material changes. The steel top surface hardness values (such as Table 7 row 1) had an average of 8 HV higher values than the initial point depth from the transverse cross-sectional cut (such as Table 7 row 2). This is suggestive that these two close measurements are affected by pitting, staining and other surface corrosion. The aluminum did not show as substantial results between the surface and initial point depth.

The transverse cross-section data had a heavily affected region of change within the first 0.4 mm from the surface for steels and 0.3 mm for aluminum. In this region, the rate of hardness change was 1.75 HV increase per mm depth from the surface for steel and 0.4 HV per mm for aluminum. The progression of these regions was significant for steel but minimal for aluminum. This hardness rate, which restated, is the change of hardness per unit distance from the surface, is depicted in progressive exposure Table 14.

This table helps to conclude some relevant conclusions:

- Steel surfaces exposed to this wet irradiated environment will deplete a small depth of the surface quicker with more exposure. Less dramatic changes occur after a specific depth (0.4 mm).
- Steel surfaces may have an inherent surface to interior microstructure difference in hardness with any air exposed environment, but ultimately by a small factor and practically uniform.
- Aluminum can evolve from an empirically uniform transverse hardness to a structure with a small rate of change from the surface, however minor a value.

Table 7 Steel cross-section hardness result (post test)

Depth from surface (mm)	Lateral point measurements (in 0.2-mm increments)										Average (HV)
Surface[a] (0.0)	194	196	196	199	194	200	193	189	192	195	194.8
0.1	182	186	188	186	182	181	188	187	187	188	185.5
0.2	191	188	187	184	189	192	196	190	184	188	188.9
0.3	196	195	192	196	191	187	191	190	189	192	191.9
0.4	191	193	194	189	193	189	197	198	192	186	192.2
0.5	188	192	191	199	199	185	187	191	187	195	191.4
0.6	195	193	196	193	191	186	186	193	188	196	191.7
0.7	193	187	194	194	195	193	192	194	189	195	192.6
0.8	193	193	193	189	192	196	193	194	193	192	192.8

[a]This set of readings was completed from the top surface before the cross-section cut was made

Table 8 Aluminum cross-section hardness result (post test)

Depth from surface (mm)	Lateral point measurements (in 0.2 mm increments)										Average (HV)
Surface[a] (0.0)	102	98.9	100	103	98.9	102	98.9	100	102	100	100.57
0.1	102	98.4	101	103	102	100	103	102	100	104	101.54
0.2	106	106	106	103	103	99	101	100	104	100	102.8
0.3	106	102	113	106	103	106	102	101	106	103	104.8
0.4	103	102	105	101	103	103	102	105	103	103	103
0.5	111	103	107	107	105	109	103	107	104	103	105.9
0.6	106	102	113	106	103	106	102	101	106	103	104.8
0.7	108	103	107	105	105	109	103	102	103	103	104.8
0.8	105	103	106	105	106	102	107	102	104	103	104.3

[a]This set of readings was completed from the top surface before the cross-section cut was made

While keeping consistent to thickness specification, the longest exposure results of both hardness test data and tensile test data can present a relationship among all properties, to include dry weight, elastic modulus, UTS, and hardness measures. Tables 15, 16, 17, 18 and 19 show the summarized relationships of each property within each sample material and size for both steel and aluminum samples. Hardness depth measures were not collected on thin specimen and tensile properties were not collected for the thick steel specimen. The boldface underscored values are the strongest relationships with values over 0.7. The boldface values are the moderate relationships with values between 0.5 and 0.7.

Values were computed using the "fit to trend-line" to determine the best fit slope of each parameter. This differs from the overall percentage of change by last run because it accounts for data from previous runs. The ratio of the two slopes of each property pair is then to give the value between 0 and 1 found in the tables. A value of 1 would represent the strongest linear relationship of two properties.

The primary expectations for these relationships was to establish at minimum one strong relationship with surface hardness, since it is the most conventional and established method. The strong relationships only occurred in the steel samples but UTS relationship with elastic modulus and surface hardness was also a moderate relationship found in almost all categories. If it were not for the significant deviation in baseline aluminum UTS, it is estimated that UTS would have had a moderate relationship with surface hardness in all five of the relationships acquired. Overall, the elastic modulus was expected to have a subtle more linear change like that of hardness, so the last thick aluminum is hard to justify without more data.

Table 16 for standard steel relationships depicts the strongest relationship found which was between surface hardness and UTS. With a relationship above 0.9 of these values, it parallels the strongest relationship found in the referenced steel lifetime study in Ref. Smart and Bond (2016), which showed that the hardness and UTS has the strongest relationship at 0.960 and was one of the only three strong relationships found of the longer list of property considerations.

Weight and depth hardness also had a couple moderate relationships. Weight is likely a factor that can be misleading because it will be heavily reliant on the in-service structure and surface condition, but it is appropriate that it only related to the steel samples. The depth regions that had moderate

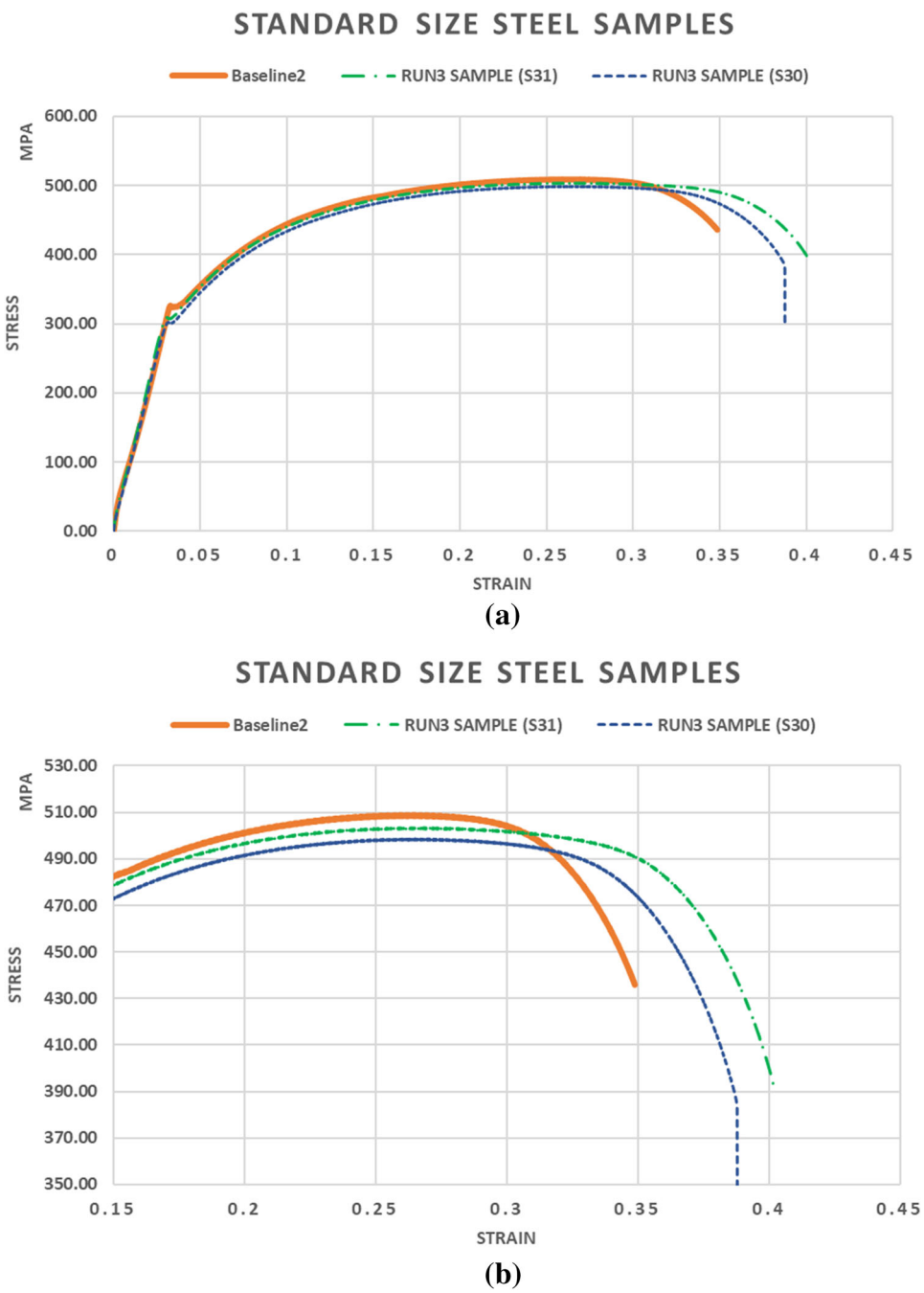

Fig. 13 **a** Stress–strain plot of standard steel, and **b** enlarged plot

relationships were not consistent. For instance, the surface to 0.4 mm had a moderate relationship with surface hardness for standard aluminum but neither of the other aluminum surface hardness. The takeaways from the depth hardness results are confined to rates given in Table 14.

The hardness data collected for this experiment were analogous to other experiments and have shown a valid relationship to the most desirable property of UTS. This should signify that conventional hardness values could be a feasible start for forecasting. The conventional hardness values were different at the surface; so, it is indeterminate if the values that produce the 0.908 relationship can foresee failure since correlations remain a relationship between local and homogenous properties. Overall, the trends appear valid along with a valid rate of change near the surface exposed to harsh environments.

The region of the material that emerged as the most noteworthy was the immediate surface of the aluminum and steel plates, with values of hardness that changed at a rate of change at 0.4 HV/mm for aluminum and 1.75 HV/mm for steel. The response to strain in these surface regions has evidence of changes that could possibly be captured

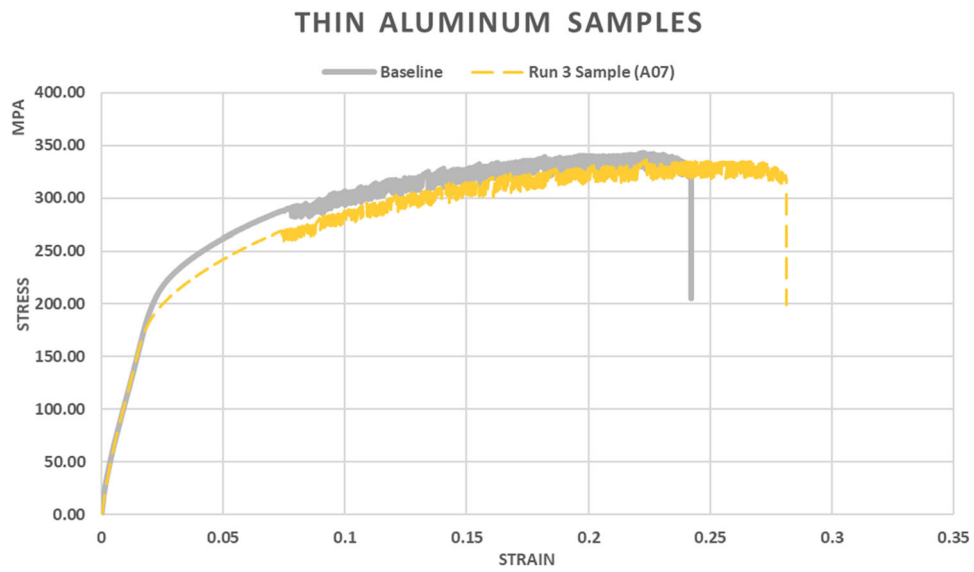

Fig. 14 Stress–strain plot of thin aluminum

Table 9 Thin aluminum ultimate tensile strength

Thin aluminum data				
Run	Average (MPa)	Change (%)	Standard deviation (MPa)	# of samples
Baseline	341.1		9.6	8
Run1 (21 days)	339.3	− 0.530	4.8	5
Run2 (50–60 days)	335.8	− 1.555	4.6	5
Run3 (100 days)	336.0	− 1.509	5.0	3

Table 10 Standard aluminum ultimate tensile strength

Standard aluminum data				
Run	Average (MPa)	Change (%)	Standard deviation (MPa)	# of samples
Baseline	365.6		11.3	8
Run1 (21 days)	368.0	0.638	6.0	5
Run2 (50–60 days)	366.6	0.252	6.3	5
Run3 (100 days)	362.8	− 0.787	1.7	3

Table 11 Thick aluminum ultimate tensile strength

Thick aluminum data				
Run	Average (MPa)	Change (%)	Standard deviation (Pa)	# of samples
Baseline	365.6		16.6	8
Run1 (21 days)	346.8	− 5.147	9.1	2
Run2 (50–60 days)	344.0	− 5.905	1.4	2
Run3 (100 days)	343.0	− 6.186	1.8	6

Table 12 Thin steel ultimate tensile strength

Thin steel data				
Run	Average (MPa)	Change (%)	Standard deviation (MPa)	# of samples
Baseline	489.5		6.8	7
Run1	485.9	− 0.735	3.8	5
Run2	486.2	− 0.669	3.2	3
Run3	482.4	− 1.453	6.2	4

Table 13 Standard steel ultimate tensile strength

Standard steel data				
Run	Average (MPa)	Change (%)	Standard deviation (MPa)	# of samples
Baseline	503.2		6.9	7
Run1	501.3	− 0.373	8.5	6
Run2	509.9	1.328	21.6	4
Run3	497.9	− 1.061	7.1	5

Table 14 Hardness rate of change per distance from the exposed surface

	Baseline (HV/mm)	100 days (HV/mm)	150 days (HV/mm)
Steel (0–0.4 mm)	0.22	1.2	1.75
Steel (0.4 mm –)	0.07	0.10	0.09
Aluminum (0–0.3 mm)	0.02	0.4	
Aluminum (0.3 mm –)	0.01	0.3	

Table 15 Thin steel relationships

	Thin samples					
	Surface hardness	Depth hardness (surface to 0.4 mm)	Depth hardness (0.4 mm +)	UTS	Elastic modulus	WT
Surface hardness				**0.610**	0.500	0.328
Depth hardness (surface to 0.4 mm)						
Depth hardness (0.4 mm +)						
UTS	**0.610**				***0.800***	0.200
Elastic modulus	0.500			***0.800***		**0.625**
WT	0.328			0.200	**0.625**	

Bold and bold italics indicate important values compared to others

Table 16 Standard steel relationships

	Standard samples					
	Surface hardness	Depth hardness (surface to 0.4 mm)	Depth hardness (0.4 mm +)	UTS	Elastic modulus	WT
Surface hardness		**0.507**	0.231	***0.908***	0.462	**0.539**
Depth hardness (surface to 0.4 mm)	**0.507**		0.454	**0.559**	**0.606**	0.344
Depth hardness (0.4 mm +)	0.231	0.454		0.254	***0.750***	0.156
UTS	***0.908***	**0.559**	0.254		**0.508**	**0.614**
Elastic modulus	0.462	**0.606**	***0.750***	**0.508**		0.208
WT	**0.539**	0.344	0.156	**0.614**	0.208	

Bold and bold italics indicate important values compared to others

Table 17 Thin aluminum relationships

	Thin samples					
	Surface hardness	Depth hardness (surface to 0.4 mm)	Depth hardness (0.4 mm +)	UTS	Elastic modulus	WT
Surface hardness				**0.537**	**0.602**	0.379
Depth hardness (surface to 0.4 mm)						
Depth hardness (0.4 mm +)						
UTS	**0.537**				0.370	0.204
Elastic modulus	**0.602**			0.370		0.092
WT	0.379			0.204	0.092	

Bold and bold italics indicate important values compared to others

Table 18 Standard aluminum relationship

	Standard samples					
	Surface hardness	Depth hardness (surface to 0.4 mm)	Depth hardness (0.4 mm +)	UTS	Elastic modulus	WT
Surface hardness		0.263	**0.579**	**0.559**	**0.633**	0.053
Depth hardness (surface to 0.4 mm)	0.263		0.250	0.147	0.250	0.200
Depth hardness (0.4 mm +)	**0.579**	0.250		0.454	**0.550**	0.090
UTS	**0.559**	0.147	0.454		**0.588**	0.029
Elastic modulus	**0.633**	0.250	**0.550**	**0.588**		0.050
WT	0.053	0.200	0.090	0.029	0.050	

Bold and bold italics indicate important values compared to others

Table 19 Thick aluminum relationships

	Thick samples					
	Surface hardness	Depth hardness (surface to 0.4 mm)	Depth hardness (0.4 mm +)	UTS	Elastic modulus	WT
Surface hardness		0.207	0.483	0.154	0.242	0.058
Depth hardness (surface to 0.4 mm)	0.207		0.429	0.032	0.050	0.283
Depth hardness (0.4 mm +)	0.483	0.429		0.074	0.117	0.121
UTS	0.154	0.032	0.074		**0.638**	0.009
Elastic modulus	0.123	0.050	0.117	**0.638**		0.014
WT	0.058	0.283	0.121	0.009	0.140	

Bold and bold italics indicate important values compared to others

if granular basis is incorporated in a hardness technique like Instrumented Indentation Technique (IIT). This method could differentiate a hardness change of grains or a factor of sensitization. Grain size was incorporated in many of the studies found in the hardness experiment genre but was only found as a mild relationship when quantified in Ref. Smart and Bond (2016). If a grain size collection was also incorporated into conventional experimental methods, it is plausible to use the conventional methods to solidify a prolonged UTS estimation.

5 Conclusions

This study, aimed to characterize the change in mechanical properties that conventional hardness testing can identify, was an extensive data collection process due to prolonged weather testing process and the variety of test methods. Distinguishing results of hardness values alone have been considered an accurate portrayal of expected changes in UTS but only with more elaborate micro-hardness equipment and software. No experiments have been found to represent an empirical study with actual exposure and advanced techniques such as IIT. Therefore, it was found appropriate to use a conventional hardness method track changes in metals alloys placed in a QUV accelerated weather chamber.

Upon collection of each exposure period and test method conclusion, some fundamental conclusions were established early. With accumulation of exposure, the hardness and UTS values from destructive and nondestructive testing both decrease in value by as much as 3% through 100 days and steel hardness by as much as 5% through 150 days. Elastic modulus changes were slightly less and less noticeable with a maximum change of 2%. The exception to these percentages was the thick aluminum samples which underwent a more significant UTS decrease and elastic modulus change, yet hardness decreased aligned with the other specimens at approximately 3%. The fluctuation of baseline properties of the thick aluminum was the likely cause to this difference and would expect to be closer aligned with the other property change relationships.

Overall, the mechanical properties of UTS and elastic modulus reflected the strongest relationships, with UTS and surface hardness sustaining the industry expected 0.9 linear relationship value. The depth hardness testing methods did not show significant relationships as did conventional surface hardness testing, but they did establish a fledgling concept of hardness heterogeneity and affected depth regions. Preliminary rates of steel hardness changes, from the surface progressing further into the depth, emerged consistent enough to establish a maximum affected region to within 0.4 mm of the surface.

Compliance with ethical standards

Conflict of interest All authors state that there is no conflict of interest.

References

ASTM E8/E8M-16a (2016) Standard test methods for tension testing of metallic materials. ASTM International, West Conshohocken

Craig BD (2005) Material failure modes, part I: a brief tutorial on fracture, ductile failure, elastic deformation, creep, and fatigue. AMPTIAC Q 9(1):9–16

Golumbfskie WJ, Tran KT, Noland JM, Park R, Stiles DJ, Grogan G, Wong C (2016) Survey of detection, mitigation, and repair technologies to address problems caused by sensitization of Al–Mg alloys on navy ships. Corrosion 72:314–328

Gouldstone A, Chollacoop N, Dao M, Li J, Minor A, Shen Y (2007) Indentation across Size scales and disciplines: recent developments in experimentation and modeling. Acta Mater 55(12):4015–4039

Kang S-K, Kim J-Y, Park C-P, Kim H-U, Kwon D (2010) Conventional Vickers and true instrumented indentation hardness determined by instrumented indentation tests. J Mater Res 25(2):337–343

Leroux P (2011) An indentation test that measures yield strength. In: Advanced materials & processes, pp 34–35

Li F, Xiang D, Qin Y, Pond RB, Slusarski K (2011) Measurements of degree of sensitization (DoS) in aluminum alloys using EMAT ultrasound. Ultrasonics 51:561–570

Lu HN, Wei DB, Jiang ZY, Liu XH, Manabe K (2013) Modelling of size effects in microforming process with consideration of grained heterogeneity. Comput Mater Sci 77:44–52

Nwokedi T, Uzoma OC, Buhari A (2018) Measuring the correlation between the tensile strength and hardness of steel and aluminum as alternative ship hull construction materials in local ship yards in Nigeria. Int J Latest Technol Eng Manag Appl Sci VII XII:51–58

Paul S (2016) Modeling unpredictable failures of 304 construction material in seawater by pitting corrosion and simulate chloride ion distribution by finite element method. Multidiscip Model Mater Struct 12(3):543–557

QUV (2019) QUV accelerated weathering tester: Q-Lab. Q-Lab. https://www.q-lab.com/products/quv-weathering-tester/quv. Accessed 8 Nov 2019

Smart L, Bond LJ (2016) Material property relationships for pipeline steels and the potential for application of NDE. In: AIP conference proceedings, vol 1706, p 160003. https://doi.org/10.1063/1.4940620

Tupper EC (2013) Introduction to naval architecture., 5th edn. Amsterdam/Elsevier, Butterworth Heinemann